Studies on Conjugated Polymers: Preparation, Spectroscopic, and Charge-Transport Properties of a New Soluble Polythiophene Derivative: Poly(3',4'-dibutyl-2,2':5'2''-terthiophene)

Chenggang Wang,† Michael E. Benz,† Eugene LeGoff,† Jon L. Schindler,‡ Joyce Allbritton-Thomas,‡ Carl R. Kannewurf,‡ and Mercouri G. Kanatzidis*,†,§

Department of Chemistry and the Center for Fundamental Materials Research, Michigan State University, East Lansing, Michigan 48824, and Department of Electrical Engineering and Computer Science, Northwestern University, Evanston, Illinois 60208-3118

Received September 20, 1993. Revised Manuscript Received January 25, 1994®

A new polythiophene derivative has been synthesized by chemical oxidative polymerization of 3',4'-dibutyl-2,2':5'2''-terthiophene (DBTT). The new polymer, poly(DBTT), contains two soluble fractions of differing molecular weights both of which were characterized by X-ray-diffraction, IR, NMR, UV-vis-NIR, photoluminescence, and ESR spectroscopies, as well as magnetic susceptibility and charge-transport measurements. The molecular weights of both fractions were determined by gel permeation chromatography. The high molecular weight fraction ($\bar{M}_w \sim 9.1 \times 10^3$) has one of the longest π-conjugation lengths known for poly(alkylthiophenes) and high conductivity. The low molecular weight fraction ($\bar{M}_w \sim 4.3 \times 10^3$) has a shorter conjugation length and 2 orders of magnitude lower conductivity ($\sim 10^{-2}$ S/cm) at room temperature. Thermal gravimetric analysis studies show that the polymer is stable in nitrogen up to 380 °C. Variable-temperature charge-transport data (conductivity and thermopower) for both doped polymer fractions indicate p-type metallic behavior. These results are compared to previously characterized polythiophenes.

Introduction

In the field of conjugated polymers polythiophenes occupy a prominent position because of their high electrical conductivity, thermal and chemical stability, amenability to chemical modification, reversible redox properties, and other interesting physical properties.[1,2] Chemical modifications on the polythiophene backbone yield processable polythiophenes.[3] Numerous applications have been demonstrated using these materials. Examples include rechargeable battery electrodes,[4] field-effect transistors,[5] electroluminescent devices,[6] and nonlinear optical devices.[7] Polythiophenes and their derivatives are prepared by either chemical or electrochemical methods.

Recently, the study of polythiophenes derived from well-defined oligomers has attracted increased attention.[8-10] The main goal in these studies is to exercise regio- and stereochemical control in the polymer so that undesirable thiophene ring linkages such as α,β- and β,β- are reduced.[11] In poly(3-alkylthiophenes)[8] (P3AT), the added chains can result in lower electrical conductivity than the unsubstituted polymer, due to steric hindrance which disrupts the coplanarity of the thiophene rings. Another cause of structural irregularity originates from the fact that in 3-alkylthiophene, the 2- and 5-positions are geometrically inequivalent, making possible two types of α,α-couplings. Although head-to-tail couplings are favored, 10-20% of coupling defects involve head-to-head couplings.[12] Several studies on disubstituted polythiophenes (e.g., poly(4,4'-dialkyl-2,2'-bithiophene)[13a] and poly(3,3'-dialkyl-2,2'-

† Michigan State University.
‡ Northwestern University.
§ A. P. Sloan Foundation Fellow 1991-93 and Camille and Henry Dreyfus Teacher Scholar 1993-95.

® Abstract published in *Advance ACS Abstracts,* March 1, 1994.

(1) (a) Genies, E. M.; Boyle, A.; Lapkowski, M.; Tsintavis, C. *Synth. Met.* **1990**, *36*, 139-182. (b) Kanatzidis, M. G. *Chem. Eng. News* **1990**, *Dec. 3*, 36. (c) Patil, A. O.; Heeger, A. J.; Wudl, F. *Chem. Rev.* **1988**, *88*, 183-200.

(2) Tourillon, G. In Skotheim, T. J., Ed. *Handbook of Conducting Polymers*; Marcel Dekker: New York, 1986; Vol. I.

(3) Gustafsson, G.; Inganas, O.; Salanek, W. R.; Laasko, J.; Loponen, M.; Taka, T.; Österholm, J.-E.; Stubb, H.; Hjertberg, T. In *Conjugated Polymers*; Bredas J. L., Silbey, R., Eds.; Kluwer Academic Publishers: Netherlands, 1991; pp 315-362.

(4) (a) Kaufman, J. H.; Chung, T. C.; Heeger, A. J.; Wudl, F. *J. Electrochem. Soc.* **1984**, *131*, 2092-2093. (b) Biserni, M.; Marinangeli, A.; Mastragostino, M. *J. Electrochem. Soc.* **1985**, *132*, 1597-1601. (c) Ganrnier, F.; Tourillon, G.; Gazard, M.; Dubois, J. C. *J. Electroanal. Chem. Interfacial Electrochem.* **1983**, *148*, 299-303.

(5) Tsumura, A.; Koezuka, H.; Ando, T. *Synth. Met.* **1988**, 25, 11-23.

(6) (a) Bradley, D. D. C. *Synth. Met.* **1993**, *54*, 401. (b) Friend, R.; Bradley, D.; Holmes, A. *Phys. World* **1992** *Nov*, 42-46. (c) Braun, D.; Gustafsson, G.; McBranch, D.; Heeger, A. J. *J. Appl. Phys.* **1992**, *72*, 564-568.

(7) (a) Sinclair, M.; McBranch, D.; Moses, D.; Heeger, A. J. *Synth. Met.* **1989**, *28*, D645-D653. (b) Singh, B.; Samoc, M.; Nalwa, H. S.; Prasad, P. N. *J. Chem. Phys.* **1990**, *92*, 2756-2761. (c) Houlding, V. H.; Harata, A.; Yardley, J. T.; Elsenbaumer, R. L. *Chem. Mater.* **1990**, *2*, 169-172.

(8) Roncali, J. *Chem. Rev.* **1992**, *92*, 711-738.

(9) (a) Guay, J.; Diaz, A.; Wu, R.; Tour, J. M.; Dao, L. H. *Chem. Mater.* **1992**, *4*, 254-255. (b) Guay, J.; Kasai, P.; Diaz, A.; Wu, R.; Tour, J. M.; Dao, L. H. *Chem. Mater.* **1992**, *4*, 1097-1105. (c) Faid, K.; Leclerc, M. *J. Chem. Soc., Chem. Commun.* **1993**, 962-963. (d) Tour, J. M.; Wu, R. *Macromolecules* **1992**, *25*, 1901-1907.

(10) (a) Yassar, A.; Delabouglise, D.; Hmyene, M.; Nessak, B.; Horowitz, G.; Garnier, F. *Adv. Mater.* **1992**, *4*, 490-494. (b) Hill, M. G.; Penneau, J.-F.; Zinger, B.; Mann, K. R.; Miller, L. L. *Chem. Mater.* **1992**, *4*, 1106-1113.

(11) Souto-Maior, R.; Wudl, F. *Synth. Met.* **1989**, *28*, C281-C286.

(12) (a) Zagorska, M.; Krische, B. *Polymer* **1990**, *31*, 1379. (b) Sato, M.-A.; Morii, H. *Macromolecules* **1991**, *24*, 1196-1200. (c) Leclerc, L.; Diaz, F. M.; Wegner, G. *Makromol. Chem.* **1989**, *190*, 3105-3116. (d) McCullough, R. D.; Lowe, R. D. *J. Chem. Soc., Chem. Commun.* **1992**, 70-72.

(13) (a) Zagorska, M.; Kulszewicz-Bajer, I.; Pron, A.; Firlej, L.; Bernier, P.; Galtier, M. *Synth. Met.* **1991**, *45*, 385-393. (b) Souto Maior, R. M.; Hinkelmann, K.; Eckert, H.; Wudl, F. *Macromolecules* **1990**, *23*, 1268-1279.

0897-4756/94/2806-0401$04.50/0

bithiophene)[13b]), in which the head-to-head couplings are predominant, showed significantly reduced conjugation lengths compared to the unsubstituted material.[13] Steric effects such as intrachain sulfur–alkyl repulsions become surprisingly dominant, forcing the thiophene rings out of coplanarity and thus reducing π-conjugation. Recently, significant progress has been reported in the regiospecific synthesis of ~100% head-to-tail polyalkylthiophenes which exhibit significantly higher conductivities.[14]

With the goal of obtaining a soluble conjugated polythiophene, without the irregular couplings mentioned above, we synthesized and polymerized the novel monomer 3′,4′-dibutyl-α-terthiophene (DBTT):

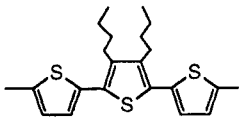

DBTT

DBTT has a known structure (a detailed X-ray diffraction single-crystal structure determination has been carried out in our laboratory).[15] The two butyl groups on the center ring are expected to enhance the solubility of the corresponding polymer in common organic solvents. However, because the two opposite α-positions of DBTT are geometrically equivalent, the problem of head-to-head vs head-to-tail coupling which is commonly seen in the polymerization of 3-alkylthiophenes is eliminated. A preliminary account of this work has appeared.[16]

Polymerization of 3,4-dialkylthiophene yields a polymer which also avoids the head-to-head vs head-to-tail coupling problem, but steric hindrance among the large number of alkyl groups does not help in achieving planarity.[17a] We also here must mention that the polymerization of an isomeric terthiophene derivative 3,3-dihexylterthiophene and several monoalkylated analogs of DBTT have been briefly described in the literature.[17] DBTT, on the other hand, is expected to produce a polymer which, because of the reduced number of side chains, minimizes extensive steric effects and thus exhibit a more coplanar backbone. In each repeating unit, more space has been provided for the extension of the two butyl groups. In addition, the lower density of the side *n*-butyl groups per thiophene ring compared to other poly(3-alkylthiophenes), in principle, could lead to a better supramolecular association of polymer chains thereby facilitating charge carrier hopping. Also, the relatively low oxidation potential of DBTT (0.86 V vs SCE) allows both chemical and electrochemical[18] polymerization under mild conditions. This avoids overoxidation and potential side reactions of the product. In this paper, we present the synthesis, chemical and molecular weight characterization, as well as X-ray diffraction, spectroscopic, magnetic, and charge transport properties of this new polythiophene derivative.

Experimental Section

Reagents. $FeCl_3$ (anhydrous), $CHCl_3$, CH_3CN, CH_3NO_2, MeOH, and I_2 were purchased from commercial sources and used as received. 2-Bromothiophene was purchased from Aldrich Chemical Co. $Pd(dppf)Cl_2$ was prepared according to ref 19a (dppf = 1,3-bis(diphenylphosphino)ferrocene).

2,5-Dibromo-3,4,-dibutylthiophene. To 18.7 g (95.4 mmol) of 3,4-dibutylthiophene[19b] was added to 66 g (210 mmol) of tetramethylammonium tribromide (TMAT) in 100 mL of 1:1 acetic/dichloromethane. The reaction was monitored by TLC and was complete in 25 min. The mixture was diluted to 200 mL with CH_2Cl_2 and filtered to remove Me_4NBr. The filtrate was washed with water (3 × 50 mL) and then with saturated $NaHCO_3$ solution until all acetic acid odor was gone. It was dried with $MgSO_4$ and the solvent was removed under reduced pressure. Purification of the crude product by flash chromatography gave 31.1 g (92%) of 2,5-dibromo-3,4,-dibutylthiophene as a clear liquid. ^1H NMR ($CDCl_3$) δ 2.5 (t, 4H), 1.1–1.3 (m, 8H), 0.95 (t, 6H); ^{13}C NMR ($CDCl_3$) δ 141.4, 107.8, 31.7, 28.7, 22.6, 13.9; EI-MS *m/z* (relative intensity) 356 (*m* + 2, 9.6), 354 (m^+, 18.9), 352 (9.1), 269 (49.6), 233 (31.8), 191 (92.8), 189 (base).

3′,4′-Dibutyl-2,2′:5′2″-terthiophene. A dry 100-mL flask containing 2.0 g of Mg was placed in an ice bath and dry ether was added to cover. To it was added dropwise 6.1 mL of 2-bromothiophene (63 mmol) in 20 mL of ether. After addition was complete, 100 mL of dry ether was added, and the solution was refluxed for 1 h. A dry 500-mL flask containing 5.4 g of 2,5-dibromo-3,4-dibutylthiophene, 100 mg of $Pd(dppf)Cl_2$[19a] (0.4 mol %), and 300 mL of dry ether was placed in a dry ice/acetone bath. The Grignard solution was transferred to this flask by a double-ended needle. The Grignard solution must be added with care to ensure that the vigorous stirring continues. The cold bath was removed and the mixture was stirred for 72 h at room temperature. It was then quenched and washed with water. The organic layer was dried with $MgSO_4$ and the solvent removed under reduced pressure. The product was purified by flash chromatography using hexanes as eluent; yield 4.58 g (83%) of the pale yellow green DBTT (mp = 36–36.5 °C). ^1H NMR ($CDCl_3$) δ 7.35 (d, 2H), 7.19 (d, 2H), 7.10 (dd, 2H), 2.77 (t, 4H), 1.61 (quintet, 4H), 1.50 (sextet, 4H), 1.00 (t, 6H); ^{13}C NMR ($CDCl_3$) δ 139.7, 135.9, 127.0, 124.9, 124.4, 123.4, 32.3, 27.1, 22.3, 13.1; EI-MS *m/z* (relative intensity) 360 (m^+, 3.63), 317 (6.4), 303 (2.56), 275 (32.4), 166 (18.8), 127 (22.74). UV (acetonitrile) λ_{max} = 331 nm (ϵ 15 000).

Preparation of Neutral Poly(3′,4′-dibutyl-2,2′:5′2″-terthiophene). To a stirred solution of 1.00 g (2.78 mmol) of DBTT dissolved in 40 mL of chloroform was added dropwise a mixture of 1.80 g (11.12 mmol) of anhydrous ferric chloride in 150 mL of chloroform. A deep blue-black precipitate appeared quickly. The resultant dark mixture was stirred at room temperature for ~48 h and then poured into 1000 mL of methanol. The resulting precipitate was filtered from the reaction mixture and exhaustively extracted with methanol in a Soxhlet extractor for 24 h in order to remove the residual oxidant and oligomers. This was followed by extraction with acetone and drying in vacuo at 50 °C for 24 h. There was obtained 0.87 g (87% yield) of red powder of poly(DBTT). Elemental analyses by EDS showed that Fe and Cl impurity was less 0.5%.

Isolation of fraction I: A sample of 0.42 g of poly(DBTT) was exhaustively extracted with ten 250-mL portions of $CHCl_3$ at 23 °C until the filtrate was colorless. The yellow orange extracts were combined and concentrated in vacuo to approximately 25 mL. To this solution 250 mL of methanol was added to precipitate a red powder, fraction I. The product was subsequently washed with methanol and dried in vacuo at 60 °C for 12 h to give 0.084 g of product (20% yield). ^1H NMR ($CDCl_3$) δ (ppm) 7.30, 7.13, 7.05, 2.73, 1.53, 1.46, 0.97; ^{13}C NMR ($CDCl_3$) δ (ppm) 140.50,

(14) (a) McCullough, R. D.; Lowe, R. D.; Jayaraman, M.; Anderson, D. L. *J. Org. Chem.* **1993**, *58*, 904–912. (b) McCullough, R. D.; Williams, S. P. *J. Am. Chem. Soc.* **1993**, *115*, 11608–11609. (c) McCullough, R. D.; Tristam-Nagle, S.; Williams, S. P.; Lowe, R. D.; Jayaraman, M. *J. Am. Chem. Soc.* **1993**, *115*, 4910–4911.

(15) Liao, Benz, M.; LeGoff, E.; Kanatzidis, M. G. *Adv. Mater.* **1994**, *6*, 135–138.

(16) Wang, C.; Benz, M. E.; LeGoff, E.; Schindler, J. L.; Kannewurf, C. R.; Kanatzidis, M. G. *Polym. Prepr. (Am. Chem. Soc., Polym. Chem. Div.)* **1993**, *34*, 422–423.

(17) (a) Tourillon, G.; Garnier, F. *J. Electroanal. Chem.* **1984**, *161*, 51–58. (b) Gallazzi, M. C.; Castellani, L.; Zerbi, G. *Synth. Met.* **1991**, *41–43*, 495–498. (c) Ferraris, J. P.; Newton, M. D. *Polymer* **1992**, *33*, 391–397. (d) Anderson, M. R.; Pei, Q.; Hjertberg, T.; Inganas, O.; Wennerstrom, O.; Österholm, J.-E. *Synth. Met.* **1993**, *55–57*, 1227–1231.

(18) Glenis, S.; Wang, C.; Benz, M. E.; LeGoff, E.; Schindler, J. L.; Kannewurf, C. R.; Kanatzidis, M. G., manuscript in preparation

(19) (a) Hayashi, T.; Konishi, M.; Kobori, Y.; Kumada, M.; Higuchi, T.; Hirotsu, K. *J. Am. Chem. Soc.* **1980**, *106*, 158. (b) Tamao, K.; Kodama, S.; Nakajima, I.; Kumada, M. *Tetrahedron* **1982**, *38*, 3347–3354.

136.96, 136.26, 135.41, 129.98, 129.78, 127.33, 126.58, 126.07, 125.40, 123.94, 32.86, 28.00, 23.03, 13.81.

Isolation of fraction II: The insoluble material obtained from the above procedure (ca. 0.33 g) was heated in a sealed thick-wall Pyrex tube with 300 mL of $CHCl_3$ at 80 °C for 10 h. Subsequently the tube was opened and the insoluble material was removed by filtration. The red $CHCl_3$ extract was evaporated to dryness in vacuo to afford 0.24 g of a red product, fraction II; yield 57%. ^1H NMR ($CDCl_3$) δ (ppm) 7.20, 7.12, 7.05, 2.73, 1.53–1.46, 0.97.

Preparation of Doped Poly(DBTT). (*a*) *Doping with iodine in nitromethane*: To a stirred solution of excess iodine in 50 mL of nitromethane, 0.05 g of red powder of poly(DBTT) was added. The red powder turned black immediately. After stirring for 9 h, the black solid was collected, washed several times with nitromethane, and vacuum dried. The yield was quantitative.

(*b*) *Doping with ferric chloride in nitromethane*: To a stirred solution of 0.1 M ferric chloride in 50 mL of nitromethane at room temperature was added 0.03 g of poly(DBTT). A black product formed immediately. After stirring for 12 h, the black solid was collected from the reaction mixture, washed several times with nitromethane and vacuum dried.

Physicochemical Measurements. Elemental analyses (S, Fe, Cl, I) were performed on a JEOL JSM-35C scanning electron microscope (SEM) equipped with a Tracor Northern energy dispersive spectroscopy (EDS) detector. Infrared spectra were recorded on pressed KBr pellets on a Nicolet 740 FTIR spectrometer. UV–vis–NIR absorption spectra were obtained from a Shimadzu UV-3101PC double-beam, double-monochromator spectrophotometer.

X-ray powder diffraction patterns were collected at room temperature on a Rigaku powder diffractometer using Cu Kα radiation generated by a rotating anode operating at 45 kV and 100 mA. The data were collected at a rate of 1°/min. FeOCl was used as a standard for estimating the instrumental line broadening in our Scherrer calculations.[20]

Nuclear magnetic resonance spectra (^1H and ^{13}C) were obtained using a computer controlled Varian VXR NMR (500 MHz) spectrometer. The chemical shifts are reported in parts per million (δ, ppm) using the residual solvent resonance peak as reference ($CHCl_3$, δ 7.24 ppm for ^1H and 77.00 ppm for ^{13}C).

Photoluminescence spectra were measured at room temperature on a Perkin-Elmer LS-5 fluorescence spectrophotometer. Thermogravimetric analysis (TGA) and differential scanning calorimetry (DSC) were performed on Shimadzu TGA-50 and DSC-50 under nitrogen or oxygen at a 5 or 3 °C/min heating rate. Electron spin resonance (ESR) measurements were conducted on a Bruker ER200 ESR spectrometer. Variable-temperature magnetic susceptibility measurements were carried out using a Quantum Design Inc. SQUID magnetic property measurement system (MPMS). The magnetization of each sample was examined and was found to vary linearly as a function of applied field (from 500 to 5000 G). Diamagnetic corrections were made for both the container used (plastic bag) and the contributions of the atoms in the molecule using the Pascal constants.[21]

Molecular weight measurements of the soluble fractions of poly(DBTT) were carried out using gel permeation chromatography (GPC) using a Shimadzu LC-10AS high-pressure liquid chromatograph (HPLC) equipped with a PL-GEL 5 μm (MIXED-B) column of length 300 mm. Chromatographic grade tetrahydrofuran (THF) was used as an eluent. Calibration was made with a series of polystyrene standards ($\bar{M}_w$ in the range 3 250–500 800).

Charge-Transport Measurements. Dc electrical conductivity and thermopower measurements were made on pressed polymer pellets. Conductivity measurements were performed in the usual four-probe geometry with 60- and 25-μm diameter gold wires used for the current and voltage electrodes, respectively. Measurements of the sample cross-sectional area and voltage probe separation were made with a calibrated binocular microscope. Conductivity data were obtained with the computer-automated system described elsewhere.[22] Thermoelectric power (TP) measurements were made by using a slow ac technique[22] with 60-μm gold wires used to support and conduct heat to the sample, as well as to measure the voltage across the sample resulting from the applied temperature gradient. Samples were suspended between the quartz block heaters by 60-μm gold wires thermally grounded to the blocks with GE 7031 varnish. The magnitude of the applied temperature gradient was generally 1.0 K. Smaller temperature gradients gave essentially the same results but with somewhat lower sensitivity.

In both measurements, the gold electrodes were held in place on the sample with a conductive gold paste. Mounted samples were placed under vacuum (10^{-3} Torr) and heated to 320 K for 2–4 h to cure the gold contacts. For a variable-temperature run, data (conductivity or thermopower) were acquired during sample warming. The average temperature drift rate during an experiment was kept below 0.3 K/min. Several variable-temperature runs were carried out for each sample to ensure reproducibility and stability. At a given temperature, reproducibility was within ±5%.

Results and Discussion

Poly(DBTT) was synthesized by direct chemical oxidative polymerization of DBTT with ferric chloride as the oxidant in chloroform, according to eq 1. The as-made

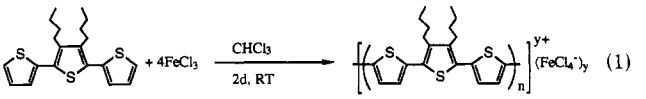

(1)

black conductive polymer is doped with $FeCl_4^-$ ($y = 0.4$). Undoping can be accomplished by Soxhlet extraction with methanol and acetone, yielding a red product.

The neutral poly(DBTT) is partly soluble in chloroform, at room temperature, giving a yellow-orange solution from which fraction I can be obtained. The room-temperature insoluble residue of poly(DBTT) is soluble in chloroform at an elevated temperature (e.g., 80 °C) giving fraction II. Finally, a small fraction is insoluble in all organic solvents, fraction III. In contrast, due to the high content of *n*-alkyl groups, P3AT are completely soluble. These fractions must differ from one another in molecular weight. The fractionation process is shown in Scheme(1). Free-standing films can be easily cast from solution by slow solvent evaporation. The films can be doped with either iodine vapor in a closed chamber or ferric chloride in nitromethane.

The expectation that the DBTT monomer would yield an ordered product was confirmed by X-ray scattering which shows that both soluble fractions are polycrystalline, when undoped. Annealing the samples at 180 °C for 15 h followed by cooling to 50 °C at 26 °C/h increased the crystallinity significantly, as shown in the powder patterns of Figure 1. The most notable feature is the intense low-angle reflection at 17.06 Å (in both fractions) and the very broad high-angle reflection at 4.40 Å. Annealing not only increased the intensity of the first low-angle reflection but also shifted it to higher 2θ angle, indicating a slight contraction of the repeating length to 16.43 and 16.74 Å for fractions I and II, respectively. Annealing also revealed clearly the presence of the second and third order reflections at 8.15 and 5.42 Å and 8.36 and 5.51 Å for fractions I and II, respectively. These peaks are attributed

(20) West, A. R. *Solid State Chemistry and Its Applications*; John Wiley and Sons: Chichester, 1984; p 173.

(21) Drago, R. S. In *Physical Methods in Chemistry*; W. B. Saunders: Philadelphia, 1977; pp 413–414.

(22) (a) Lyding, J. W.; Marcy, H. O.; Marks, T. J.; Kannewurf, C. R. *IEEE Trans. Instrum. Meas.* **1988**, *37*, 76–80. (b) Marcy, H. O.; Marks, T. J.; Kannewurf, C. R. *IEEE Trans. Instrum. Meas.* **1990**, *39*, 756–760.

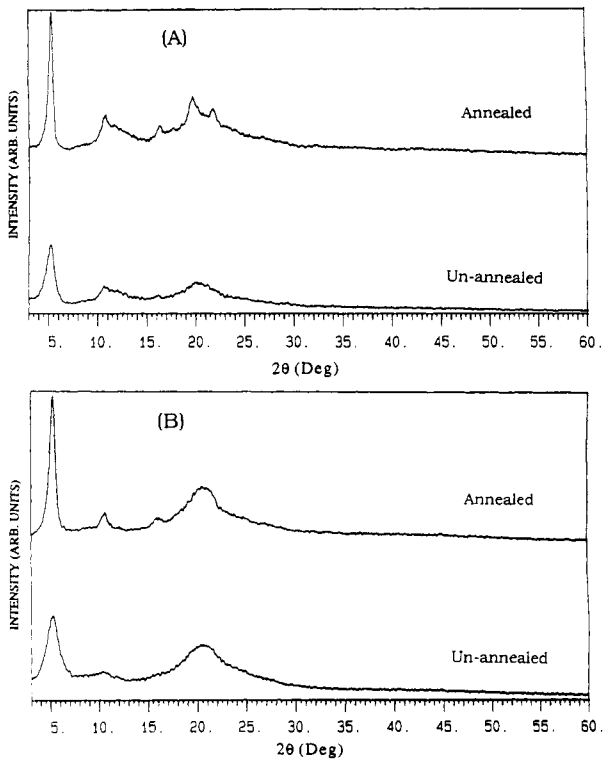

Figure 1. X-ray powder diffraction profiles for annealed and unannealed samples of (A) fraction I and (B) fraction II.

Scheme 1. Fractionation of Poly(DBTT).

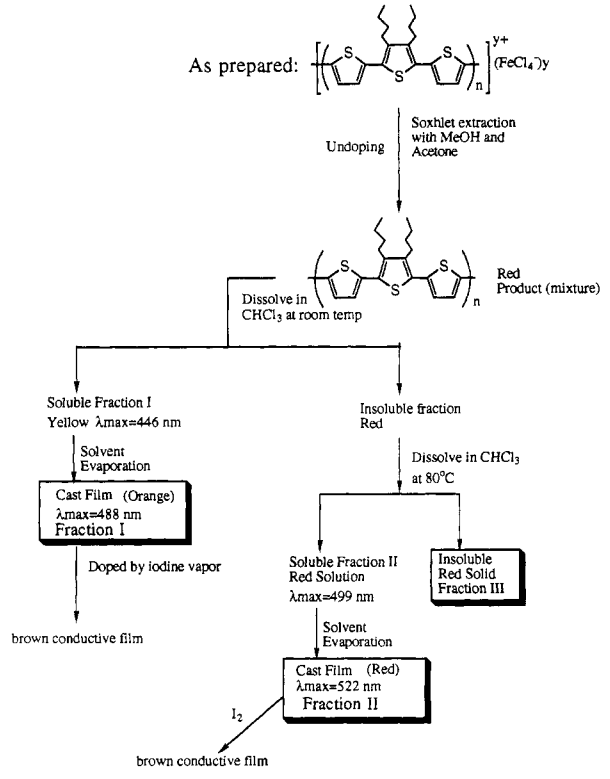

to considerable coherent ordering of the polymer chains due to their planar configuration. These reflections arise from the packing of poly(DBTT) chains which is dominated by the length and density of the butyl side chains. It should be noted here that these X-ray diffraction patterns bear strong similarities to those of P3AT and thus are likely due to the similar overall fundamental packing of alkyl-substituted thiophenes, including poly(DBTT).[23] The presence of rotational defects along the backbone, resulting from 180° rotations of the thiophene rings, particularly among those with no alkyl substitution, is entirely possible. However, the quality of the X-ray data is not sufficient to detect them. The broad peak at 3.8 Å observed in P3AT is attributed to an interlayer spacing arising from a lamellar packing of the polymer chains. It corresponds to the 4.4-Å feature observed in the diffraction pattern of poly(DBTT). The average coherence length of the unannealed fractions I and II was calculated from the Scherrer formula[20] to be 69.5 and 41 Å, while in the annealed samples it increased to 144 and 109 Å, respectively.

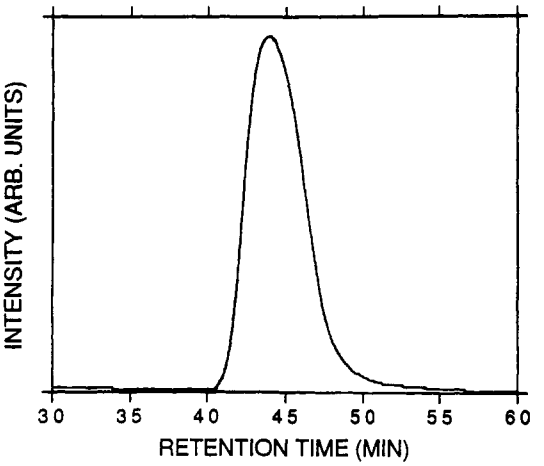

Figure 2. Typical GPC trace of fraction II of poly(DBTT) in THF solution at room temperature.

The chemical structure and properties of the polymer were further examined with vibrational, optical, NMR, and EPR spectroscopies. Photoluminescence spectroscopy was also used to explore the excited state properties of poly(DBTT). The molecular weights of the soluble fractions were determined by the GPC technique.

Chromatographic Molecular Weight Studies. Molecular weights of the two soluble fractions of poly(DBTT) were determined by gel permeation chromatography in THF. Figure 2 shows a typical chromatogram representing the molecular weight distribution from fraction II. The molecular weights were obtained from the common method of a retention time calibration curve using a series of polystyrene standards with a UV–vis detector set at 450 nm. The weight-average molecular weight ($\bar{M}_w$) of fraction I is $\sim 4.3 \times 10^3$ and number-average molecular weight ($\bar{M}_n$) is $\sim 2.6 \times 10^3$ giving a polydispersity index (PD) of 1.65. The $\bar{M}_n$ corresponds to an average of 21 rings/chain. This is in good agreement with the value obtained for this fraction by end-group analysis using NMR spectroscopy (see below). For fraction II, $\bar{M}_w$ is $\sim 9.1 \times 10^3$ and $\bar{M}_n$ is $\sim 5.7 \times 10^3$ with PD of 1.60. The $\bar{M}_n$ corresponds to 48 rings/chain. The rather small value of polydispersity indicates narrow molecular weight distribution in both soluble fractions of the poly(DBTT). We note that the measured molecular weights are an order of magnitude lower than those reported for poly(3-hexylthiophene)

(23) (a) Prosa, T. J.; Winokur, M. J.; Moulton, J.; Smith, P.; Heeger, A. J. *Macromolecules* **1992**, *25*, 4364–4372. (b) Winokur, M. J.; Spiegel, D.; Kim, Y.; Hotta, S.; Heeger, A. J. *Synth. Met.* **1989**, *28*, C419–C426. (c) Chen, S.-A.; Ni, J.-M. *Macromolecules* **1992**, *25*, 6081–6089. (d) Mardelen, J.; Samuelsen, E. J.; Gautun, O. R.; Carlsen, P. H. *Synth. Met.* **1992**, *48*, 363–380.

Table 1. Comparison of Infrared Band Positions (cm^{-1}) and Their Assignments for Poly(DBTT) and Various Poly(3-alkylthiophenes)

sample	arom C_β–H str	aliph C–H str	ring str	methyl def	arom C–H out-of-plane
poly(DBTT)	3062	2951, 2925, 2856	1492, 1456	1377	788
PTh[a]	3063		1491, 1453, 1441	1377	788
P3BT[a]	3055	2955, 2928, 2858	1512, 1458, 1439	1377	829
P3HT[a]	3055	2959, 2930, 2858	1512, 1458, 1439	1377	825

[a] See ref 24: PTH, polythiophene; P3BT, poly(3-butylthiophene); P3HT, poly(3-hexylthiophene).

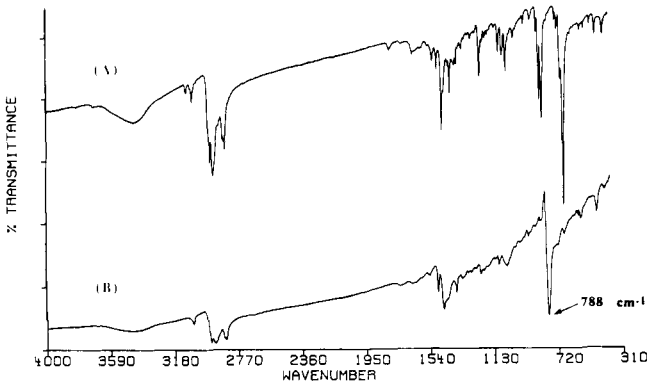

Figure 3. FT-IR transmission spectra (KBr pellets) of (A) DBTT (B) neutral poly(DBTT).

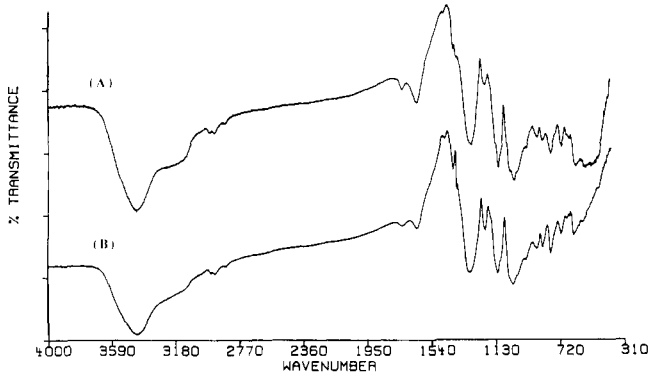

Figure 4. FT-IR transmission spectra (KBr pellets) of the doped polymer: (A) neutral poly(DBTT) doped with $FeCl_3$ in CH_3NO_2 solution; (B) neutral poly(DBTT) doped with I_2 in CH_3NO_2 solution.

(P3HT) and similar polythiophenes.[24] However, a superior polydispersity index is achieved in poly(DBTT). P3HT has $\bar{M}_w \sim 1.4 \times 10^5$ and $\bar{M}_n \sim 3.2 \times 10^4$, corresponding to a polydispersity index of 4.4.[13b] The lower MW of poly(DBTT) is in agreement with what was found for polythiophene synthesized from terthiophene. This was attributed to the increased stability of the radical cations formed from terthiophene, which slows the polymerization rate and leads to low molecular weight polymers.[17b,25] The GPC studies on the two soluble fractions of poly(DBTT) place a lower limit on the molecular weight of the completely insoluble fraction III which is expected to be much higher than 10^4.

Infrared Spectroscopy. Figure 3 shows the infrared spectra of the starting oligomer DBTT and the neutral poly(DBTT). The principal IR absorption bands observed in poly(DBTT) and their assignments, together with the corresponding results for polythiophene and P3AT, are listed in Table 1. Both fractions I and II have very similar infrared spectra with peaks at essentially the same energies but with small differences in intensity.

The strong, sharp absorption band at 788 cm^{-1} (C–H out-of-plane vibration) is characteristic of an α,α-coupled alkyl-substituted polythiophene ring, suggesting a linear polymer chain structure.[2,24] The single broad peak at 3062 cm^{-1} is due to C_β–H stretching modes. The C_α–H stretching mode, observed in the spectrum of DBTT at 3103 cm^{-1}, is absent. This provides further support for the predominance of α,α- couplings in the polymer backbone.[24] It is noteworthy that in poly(DBTT) only two bands are observed at 1456 and 1492 cm^{-1}, which are assigned to the C=C symmetric and antisymmetric stretching modes respectively. In the case of P3ATs, three bands are present in the same region (1520–1440 cm^{-1}).[24] The decrease in the number of active modes in the C=C region is probably due to the existence of an inversion center in the poly(DBTT). Similar features have been reported for poly(4,4′-dialkyl-2,2′-bithiophene)[13a] and poly(3,3′-dihexyl-2,2′-bithiophene),[13b] which also contain an inversion center in their ideal structures.

On the basis of a previous analysis of the vibrational spectra of polythiophenes and oligomers, the intensity ratio of the symmetric stretch at 1456 cm^{-1} to the asymmetric stretch at 1492 cm^{-1} (I_{sym}/I_{asym}) is indicative of the degree of conjugation in the polymer backbone.[26] Extended backbone conjugation results in small ratios. Thus, it would be interesting to compare this ratio in the two soluble fractions of poly(DBTT). The IR spectra of these fractions show clearly that I_{sym}/I_{asym} is greater in fraction I, consistent with a smaller conjugation length, as expected.

The IR spectra of the doped polymer are virtually independent of dopant and are shown in Figure 4. As in other polythiophenes, doping causes a profound change in the IR spectra due to dramatic changes in the electronic structure of poly(DBTT).

Electronic Spectroscopy, UV–Visible–NIR. The optical absorption spectra of fractions I and II, in chloroform, are shown in Figure 5. In both fractions of poly(DBTT), the energy of π–π^* transition occurs at lower energy than that observed for P3HT (maximum absorption at 439 nm in chloroform[13b]). The corresponding solution-cast films show absorption maxima at 488 nm for fraction I and 522 nm for fraction II at room temperature, see Figure 6. The higher λ_{max} and lower solubility of fraction II together suggest it has a considerably longer effective conjugated chain length and larger molecular weight. This conclusion is consistent with the molecular weight data obtained by GPC.

A red shift of the π–π^* absorption band, in going from solution to the solid state, is characteristic of all soluble polythiophenes.[1,8] This can be attributed to conforma-

(24) (a) Hotta, S.; Rughooputh, S. D. D. V.; Heeger, A. J.; Wudl, F. *Macromolecules* **1987**, *20*, 212–215. (b) Elsenbaumer, R. L.; Jen, K. Y.; Oboodi, R. *Synth. Met.* **1986**, *15*, 169–174.

(25) Roncali, J.; Garnier, F; Lemaire, M; Garreau, R. *Synth. Met.* **1986**, *15*, 323–331.

(26) Furukawa, Y.; Akimoto, M.; Harad, I. *Synth. Met.* **1987**, *18*, 151–156.

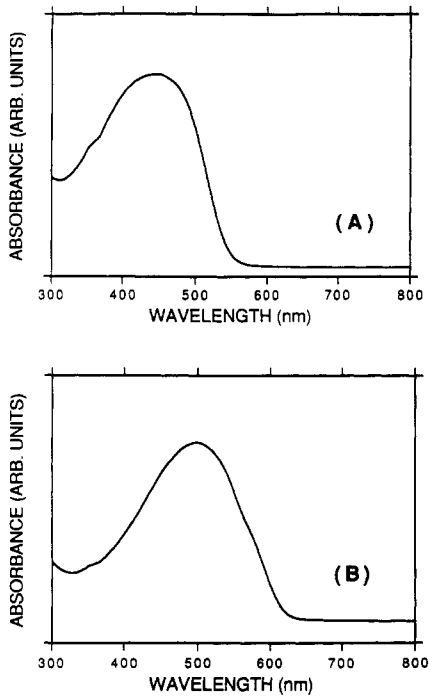

Figure 5. Solution UV–vis absorption spectra of two soluble fractions of poly(DBTT) in chloroform solution at room temperature: (A) fraction I (λ_{max} = 446 nm); (B) fraction II (λ_{max} = 499 nm).

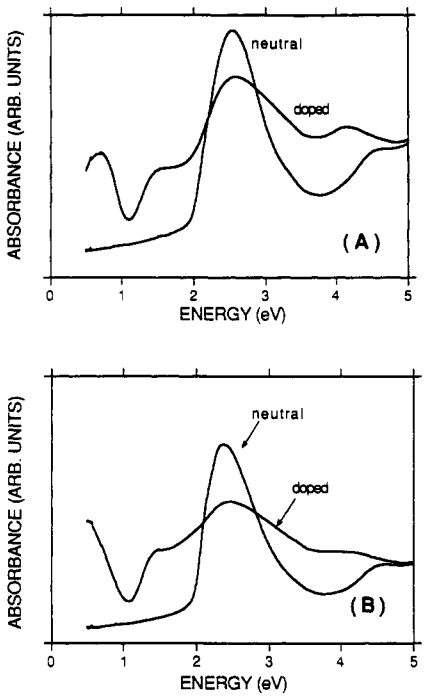

Figure 6. UV–vis–NIR absorption spectra of neutral and doped poly(DBTT) films at room temperature: (A) fraction I; (B) fraction II.

tional changes, which decrease the degree of conjugation in the polymer backbone in solution, as compared to the condensed state.[27,28] This decrease in conjugation results from the deviation of adjacent thiophene rings from coplanarity. Of course, a very small contribution to the red shift would come from the alky substituents on the backbone. It has been proposed that, in solution, polythiophenes adopt a coillike conformation resulting in relatively small conjugation lengths.[13b,24a] In the solid state a rodlike structure is expected providing a more extensive delocalization. It is notable that the shifts of the absorption maximum for the two poly(DBTT) fractions are smaller (42 and 23 nm, respectively) than in the case of P3HT (69 nm).[13b] The higher λ_{max} in solution, coupled with the smaller blue shift in going from the solid to the solution phase, indicate a considerably smaller coillike contribution to the structure of poly(DBTT) and thus less extensive deviation from coplanarity of the thiophene rings. As a result, we conclude that the average conjugated chain length in poly(DBTT) is longer than that in the typical P3AT. The conjugation length in our polymer approaches that of the 100% head-to-tail P3AT reported recently.[14] This is consistent with the fact that two-thirds of the heterocyclic rings are not alkylated and thus experience minimal steric repulsion. This justifies our initial expectations in choosing DBTT as the monomer.

At first glance, it would seem that the longer π-conjugation length in poly(DBTT) compared to P3AT, suggested by the electronic spectra, are in contrast with the molecular weight studies, which suggest correspondingly shorter overall chain lengths. The reason probably lies in the considerably more planar organization of poly(DBTT) chains resulting from reduced steric repulsion as explained above. Therefore, poly(DBTT) is the first polythiophene which exhibits longer effective conjugation lengths than P3AT while possessing smaller MW (i.e., shorter polymer chain lengths).

From the solid-state electronic spectra the bandgaps of the semiconducting poly(DBTT) fractions were determined by extrapolating the linear portions of $(\alpha h\nu)^2$ vs E plots to $(\alpha h\nu)^2 \rightarrow 0$. Interestingly, these direct bandgaps are virtually the same for fractions I and II and very similar to P3AT, suggesting that interchain π–π^* solid-state interactions must contribute significantly to the bandgap.

Upon doping with iodine, the solution cast films turn dark brown. The UV–vis–NIR absorption spectra of films for the neutral and doped state are compared in Figure 6. For a film of fraction I, the π–π^* absorption band at 2.64 eV loses intensity upon oxidation and shifts to slightly higher energy, while two new subgap absorption bands appear at 0.66 and 1.55 eV. For fraction II, the π–π^* absorption band also weakens, while two new subgap absorptions appear at 0.49 and 1.47 eV. The two midgap absorptions which develop in both cases correspond to transitions associated with the two localized bipolaron energy levels that appear within the bandgap upon doping.[1c,8] These results are consistent with charge storage predominantly in bipolarons[1c] and follow the same trends as P3AT. Further support for the conclusion that fraction II possesses a longer average conjugation length than fraction I derives from the lower energies associated with the midgap transitions of the former.

Photoluminescence Spectroscopy. Figure 7 shows the photoluminescence spectra of the two soluble fractions of poly(DBTT) in chloroform at 23 °C using excitation wavelength of 400 nm. Photoexcitation of these polymers results in broad band luminescence (half-width ~ 0.20 eV) with a peak maximium at 2.23 eV (557 nm) for fraction I and a similar band (half-width ~ 0.15 eV) with peak maximum at 2.00 eV (620 nm) for fraction II. The peak

(27) Rughooputh, S. D. D. V.; Hotta, S.; Heeger, A. J.; Wudl, F. *J. Polym. Soc., Polym. Phys. Ed.* **1987**, *25*, 1071–1078.
(28) Inganas, O.; Salaneck, W. R.; Osterholm, J.-E.; Laakso, J. *Synth. Met.* **1988**, *22*, 395–406.

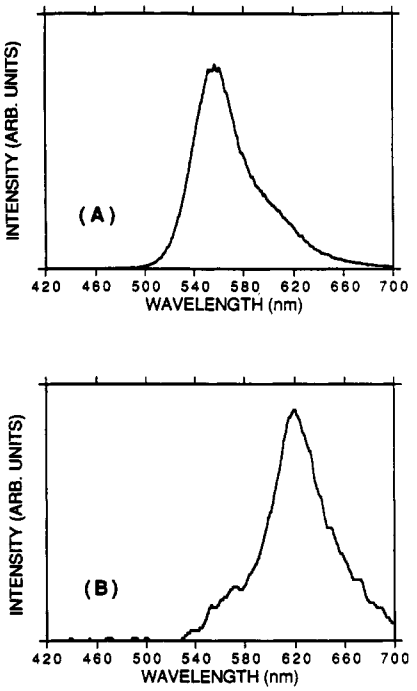

Figure 7. Photoluminescence emission spectra of two soluble fractions in chloroform solution at room temperature: (A) fraction I (λ_{max} = 557 nm); (B) fraction II (λ_{max} = 620 nm).

at 2.00 eV coincides with the onset of optical absorption of this fraction, indicating that it is a localized excitation.[29] The shift of the emission peak maximum to lower energies in fraction II parallels a similar shift of the absorption maximum seen in the electronic absorption spectra of Figure 5. This is consistent with a longer effective conjugation length in fraction II. The energy and profile of the luminescence bands are insensitive to the excitation frequency in the range of 350–500 nm for both soluble-fractions of poly(DBTT). By comparison, P3HT shows a peak at ~2.17 eV (571 nm) and half-width of 0.3 eV.[30]

In the solid state, both fractions emit light at lower energies (at 596 nm for fraction I and at 602, 627, and 656 nm for fraction II). This is in good agreement with the decrease in bandgap observed in the absorption spectra of the solids. By comparison solid films of P3HT emit at 596 nm. The photoluminescent property of the soluble fractions of poly(DBTT) offers an opportunity to study electroluminescence in these materials.[31]

NMR Spectroscopy. The polymer fractions were studied by solution 500-MHz ^{1}H NMR and 75.4-MHz ^{13}C NMR spectroscopy. The spectra of fractions I and II with their assignments are shown in Figure 8. Fraction I shows three major peaks in the aromatic region. The weak resonance at 7.30 ppm is attributed to the hydrogen atoms on the α-position of the terminal thiophene rings. The other two resonances are due to the β-hydrogen atoms. This assignment is based on the corresponding NMR spectra of the DBTT monomer and its dimer (i.e., the hexathiophene homolog).[32] From peak integration of the two types of resonances of the terminal α-hydrogen and the β-hydrogen atoms, a molecular weight determination

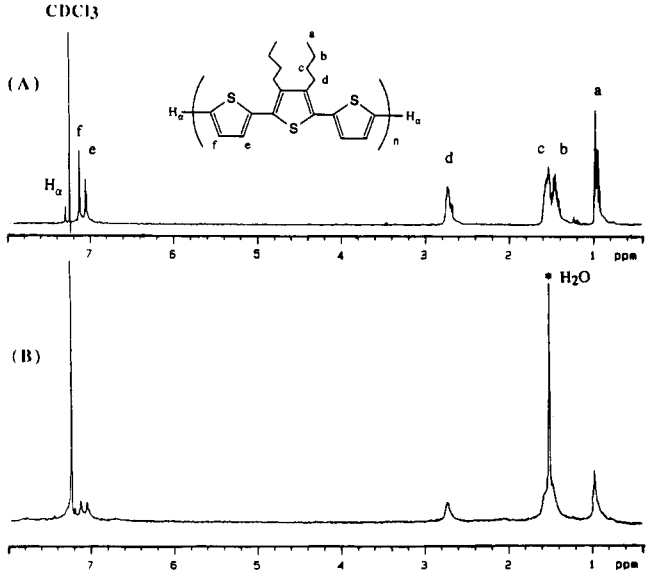

Figure 8. The 500-MHz ^{1}H NMR spectra of the two-soluble fractions of poly(DBTT) at room temperature (in $CDCl_3$): (A) fraction I; (B) fraction II. The peak integration associated with peaks f and e gives 1:1 ratio.

by end-group analysis is possible, yielding a value of ~2200, very close to six DBTT units or ~18 thiophene rings. This number agrees reasonably well with that estimated from the GPC studies described above. In fraction II, the peak due to the terminal α-hydrogen position is almost totally suppressed, and thus no end-group analysis could be done.

The four resonance peaks found in the aliphatic region correspond to the hydrogen atoms on the side *n*-butyl groups. For fraction II, the resonance peaks in the aliphatic region are much broader and less well resolved (see Figure 8B), consistent with its much higher molecular weight.

The ^{13}C NMR spectrum of fraction I of poly(DBTT) is shown in Figure 9. It shows major resonance lines at 32.9, 28.0, and 23.0 ppm assigned to the three methylene groups of the butyl moiety, while the line at 13.8 ppm is attributed to the methyl groups of same. At least 15 lines are observed in the aromatic region and correspond to the carbons on the thiophene rings. It is known that, in polythiophene, the rings can adopt a *syn* or *anti* conformation with respect to the position of the S atoms. *Ab initio* Hartree–Fock calculations indicate that the *anti* conformation is stable by only 1.3 kcal/mol.[33] If the conjugated chain in poly-(DBTT) existed in the ideal all-*anti* conformation, we would expect from symmetry arguments a total of six resonance lines for the ring carbons. The extra peaks in the spectrum could arise either from symmetry breaking and adoption, in some segments, of the *syn* conformation, via ring flips, or from the observation of signals from terminal thiophenes, or even from occasional α,β couplings. Unequivocal assignment of each peak is not available at this stage, but it is likely that several backbone conformations are contributing. This is supported by the fact that a mixture of *syn* and *anti* conformations of thiophene rings has been observed even in the solid state in a hexathiophene derivative (i.e., the dimer of DBTT) by single-crystal X-ray diffraction.[15] The most probable site for ring-flipping or occurrence of the *syn* conformation would be where the DBTT units join. At those locations

(29) Bao, Z.; Chan, W.; Yu, L. *Chem. Mater.* **1993**, *5*, 2–3.
(30) (a) Rughooputh, S. D. D. V.; Nowak, M.; Hotta, S.; Heeger, A. J.; Wudl, F. *Synth. Met.* **1987**, *21*, 41–50. (b) Linton, J. R.; Frank, C. W.; Rughooputh S. D. D. V. *Synth. Met.* **1989**, *28*, C393–C398.
(31) Wang, C.; LeGoff, E.; Blanchard, G. J.; Kanatzidis, M. G., work in progress.
(32) Benz, M. Ph.D. Dissertation, Michigan State University, 1992.
(33) Bredas, J. L.; Street, G. B.; Themans, B.; Andre, J. M. *J. Chem. Phys.* **1985**, *83*, 1323–1329.

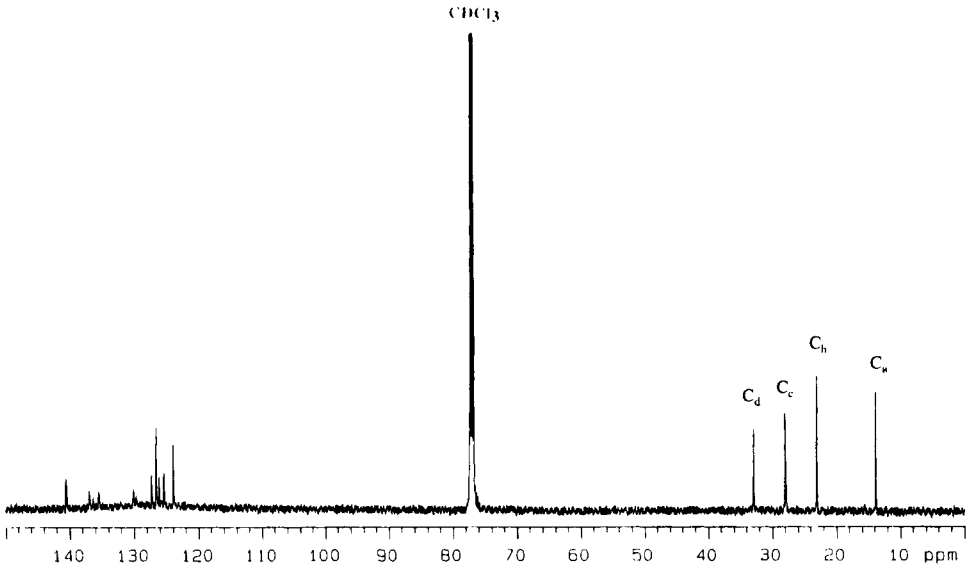

Figure 9. ^{13}C NMR spectrum of fraction I of poly(DBTT) at room temperature (in $CDCl_3$).

Chart 1

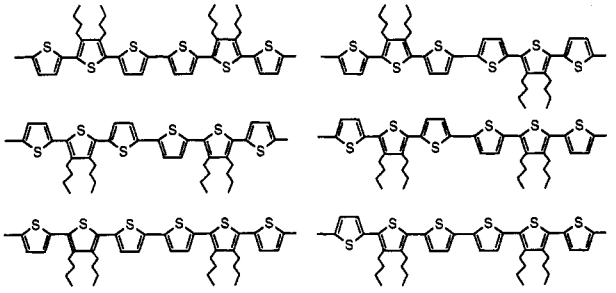

the absence of butyl groups provides the lowest rotation barrier in the polymer. Although the electronic absorption spectra discussed above do not support this possibility, the presence of α,β couplings may not be entirely ruled out. Chart 1 depicts several possibilities of coexisting *syn* and *anti* conformations. A satisfactory ^{13}C NMR spectrum of fraction II could not be obtained due to low solubility.

Thermal Analysis. The thermal stability of the polymer in its various forms was examined by thermogravimetric analysis (TGA) and differential scanning calorimetry (DSC). Neutral poly(DBTT) exhibits excellent stability in nitrogen up to at least 380 °C, as shown in the TGA data in Figure 10. In oxygen, the material starts to decompose at ~285 °C and loses 98% of its weight at 580 °C. By comparison, poly(3-octylthiophene) (P3OT) exhibits lower thermal stability, decomposing in nitrogen at 300 and in oxygen at 250 °C.[34] The greater thermal stability of poly(DBTT) is attributed to the fewer average number of alkyls groups per thiophene ring.

DSC curves of neutral poly(DBTT) show a broad, weak, endothermic peak at 236 °C, upon heating and a narrow intense exothermic peak at 207 °C upon cooling; see Figure 11. However, the polymer shows signs of no melting up to 250 °C as judged by direct visual observation, suggesting, instead, the presence of an order–disorder transition in the solid state.[23] This is supported by the increased crystallinity exhibited in the annealed samples. The changes occurring in the polymer during the heating cycles are repeatable.

(34) Gustafsson, G.; Inganas, O.; Nilsson, J. O. *Synth. Met.* **1989**, *28*, C435–C444.

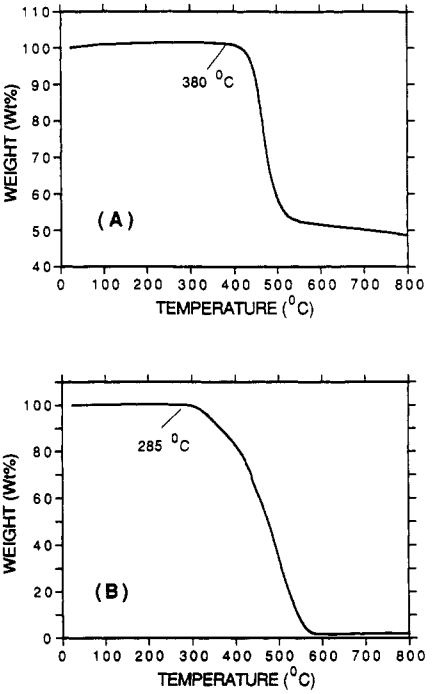

Figure 10. TGA thermograms of neutral bulk poly(DBTT): (A) under nitrogen; (B) under oxygen.

Table 2. ESR Data for Three Different Samples

sample	g factor	ΔH_{pp} (G)	spins/mol/ring	line shape
neutral poly(DBTT)	2.0033	8	3.9×10^{20}	isotropic
{poly(DBTT)$(I_3)_{0.33}$}	2.0030	26	3.5×10^{21}	anisotropic
{poly(DBTT)$(I_3)_{0.12}$}	2.0036	8	2.1×10^{21}	anisotropic

Electron Spin Resonance Spectroscopy. Electron spin resonance values for the neutral form and doped form (with different doping levels of I_3^-) of poly(DBTT) are listed in Table 2. Figure 12A shows the ESR spectrum of the neutral poly(DBTT), which reveals a single, largely symmetric, line centered at nearly the free-electron g value of 2.0033 with a line width ΔH_{pp} = 8 G. The number of spins determined, using a diphenylpicrylhydrazide (DPPH) standard, is 3.9×10^{20} spins/mol/rings, corresponding to approximately 1 spin/1544 rings. Spin quantitation performed on both fractions show a number similar to the bulk. The number of spins is about 1 order of magnitude

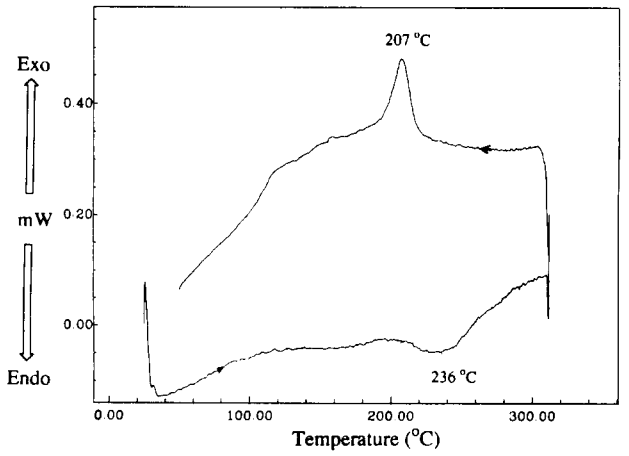

Figure 11. DSC thermogram of neutral bulk poly(DBTT) (under nitrogen).

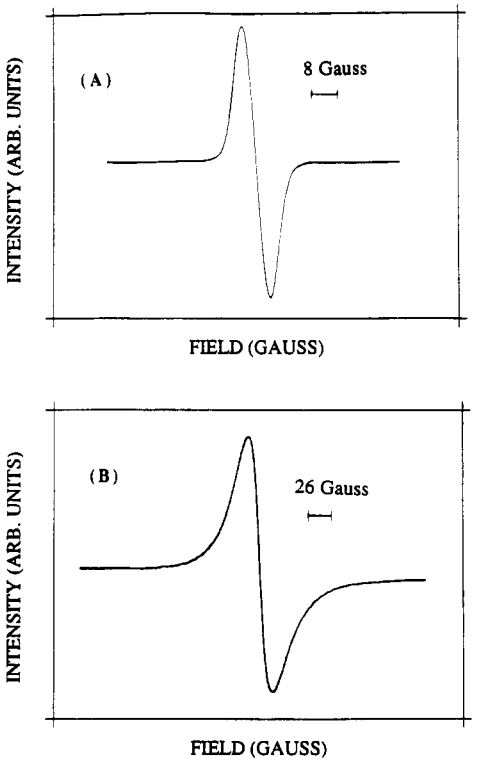

Figure 12. ESR spectra of (A) neutral bulk poly(DBTT) and (B) polymer doped with iodine (33% mol) at room temperature.

smaller than that reported for P3HT (2.4×10^{21} spins/mol[24]) and suggests a high level of purity for poly(DBTT) and fewer spin-carrying defects. This is consistent with our initial expectation that a well-designed oligomer, such as DBTT, could result in a high-quality conjugated polymer.

Figure 12B shows the ESR spectrum of iodine doped bulk poly(DBTT) (33% mol of I_3^-). A broader, single, asymmetric line with $g = 2.0030$ and $\Delta H_{pp} = 26$ G is observed, corresponding to 3.5×10^{21} spins/mol of rings. Assuming that no spin-carrying mobile carriers exist at this doping level, the larger number of spins in the doped polymer can be attributed to an increase in defect concentration during the doping process. Similar effects have been observed for P3AT.[24]

Magnetic Susceptibility Measurements. The magnetic properties of neutral and iodine-doped poly(DBTT) were investigated as a function of temperature using an applied field of 2000 G. The magnetic data are similar to

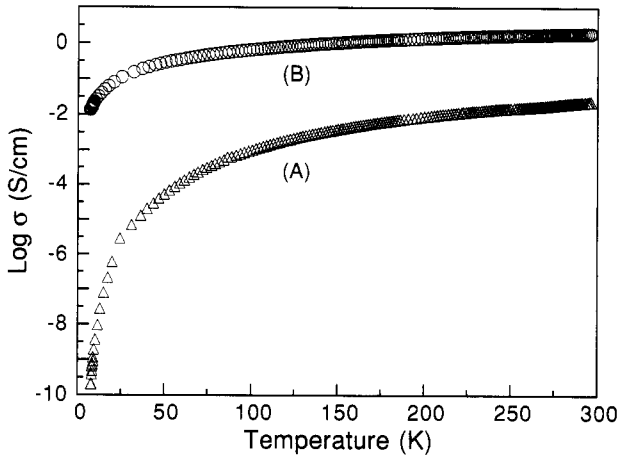

Figure 13. Four-probe variable-temperature electrical conductivity of poly(DBTT) doped with ferric chloride: (A) fraction I; (B) fraction II.

those of other polythiophenes. As observed in the ESR spectra, the neutral form shows residual paramagnetism associated with spin defects on the backbone. The magnetic susceptibility of poly(DBTT) follows Curie–Weiss law behavior as a function of temperature. The observed susceptibility (corrected for diamagnetism) is higher than that implied by ESR spectroscopy, $\sim 9.9 \times 10^{-5}$ emu/mol vs $\sim 2.4 \times 10^{-6}$ emu/mol, respectively. The higher value is attributed to the presence of residual dopant or, more likely, to inaccuracies in the diamagnetic correction, which at these low susceptibility levels is substantial.[21]

In agreement with ESR spectroscopy, the magnetic susceptibility of $\{poly(DBTT)\}(I_3)_{0.33}$ is only slightly larger that the undoped sample, $\sim 3.71 \times 10^{-4}$ emu/mol. The small rise may be attributed to an increase in the spin defects upon doping and is consistent with the presumed spinless nature of the charge carriers. However, a contribution from Pauli paramagnetism is also expected for a metallic system (see charge transport data below). When compared to the calculated magnetic susceptibility from the spin quantitation of the ESR spectra, the bulk value obtained from susceptometry is higher, probably for similar reasons given for the neutral form.

Charge-Transport Properties. *Electrical Conductivity.* The electrical conductivity of bulk poly(DBTT) (doped with $FeCl_4^-$ and iodine) has been measured by the standard four-probe method on pressed pellets as a function of temperature. Samples from the two soluble fractions doped with ferric chloride were also studied. At room temperature, fraction II and bulk poly(DBTT), doped with $FeCl_4^-$, have roughly the same conductivity of $\sim$1–5 S/cm, while fraction I is 2 orders of magnitude less conductive at $\sim$0.02–0.04 S/cm. The higher conductivity of fraction II is comparable to that of P3HT ($\sim$5–15 S/cm) chemically obtained in powder form[24] but significantly lower than that reported for the $\sim$100% head-to-tail P3AT.[14] Upon cooling these samples, the conductivity decreases only slightly for fraction II ($\sim$0.02 S/cm at 10 K) while it reaches insulator values for fraction I; see Figure 13. The conductivity measurements of poly(DBTT) were carried out as a function of iodine (I_3^-) doping. Shown in Figure 14, the highly doped polymer (33% mol I_3^-) exhibits higher conductivity, reaching 2 S/cm at 300 K, while the less doped polymer (12% mol I_3^-) has a conductivity of 0.05 S/cm at 300 K. The relatively small temperature

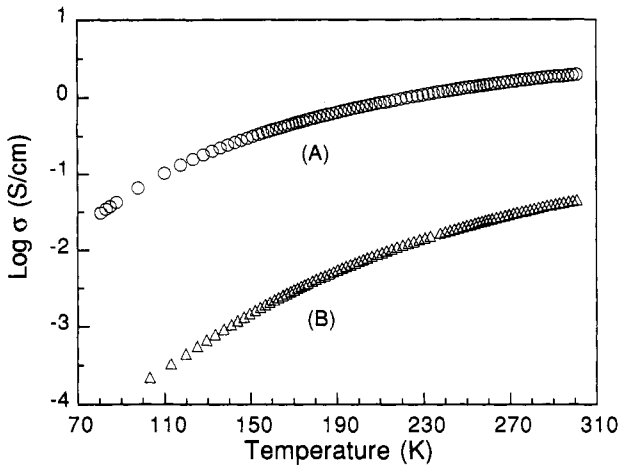

Figure 14. Four-probe variable-temperature electrical conductivity of bulk poly(DBTT) doped with iodine: (A) poly(DBTT)$(I_3^-)_{0.33}$; (B) poly(DBTT)$(I_3^-)_{0.12}$.

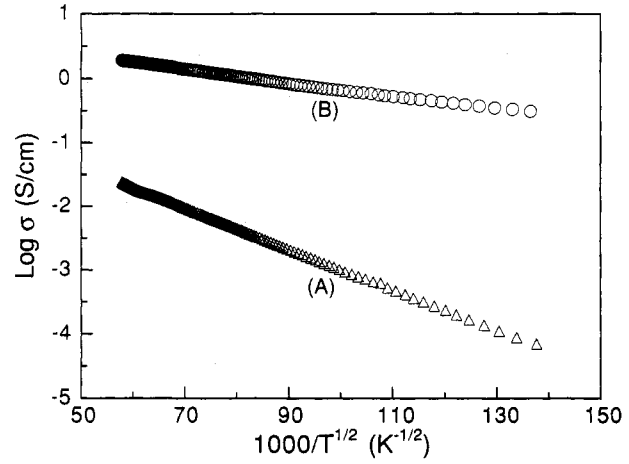

Figure 15. Four-probe variable-temperature electrical conductivity of poly(DBTT), doped with ferric chloride, in a log σ vs $T^{-1/2}$ format: (A) fraction I; (B) fraction II.

dependence of fraction II is very similar to that observed for doped polyacetylene and typical of granular metals with weak interparticle contact resistance.[35] It is possible that the conductivity of poly(DBTT) is not higher than that of P3HT, despite its longer conjugation length, because any gains in mobility from improved conjugation are offset by corresponding losses in mobility derived from the increased frequency of carrier hopping caused by the significantly shorter chain lengths in poly(DBTT). Higher conductivities could be expected if the polymer synthesis could be improved to yield higher MW material.

To gain further insight into the conduction mechanism of doped fractions I and II, we attempted to fit the experimental variable temperature data via computer analysis to the analytical expression

$$\sigma = \sigma_0 \exp[-(T_0/T)^{\alpha}]$$

where σ_0 and T are constants and $\alpha = 1, {}^1/_2, {}^1/_3$, or ${}^1/_4$ based on several conduction mechanisms suggested for such systems.[36,37] Figure 15 shows that single exponential fits

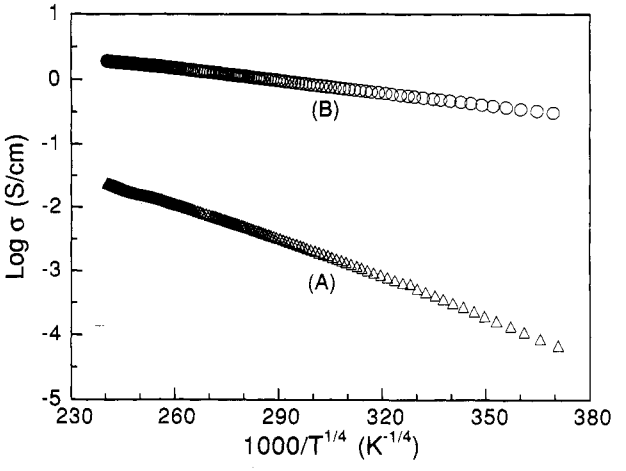

Figure 16. Four-probe variable-temperature electrical conductivity of poly(DBTT), doped with ferric chloride, in a log σ vs $T^{-1/4}$ format: (A) fraction I; (B) fraction II.

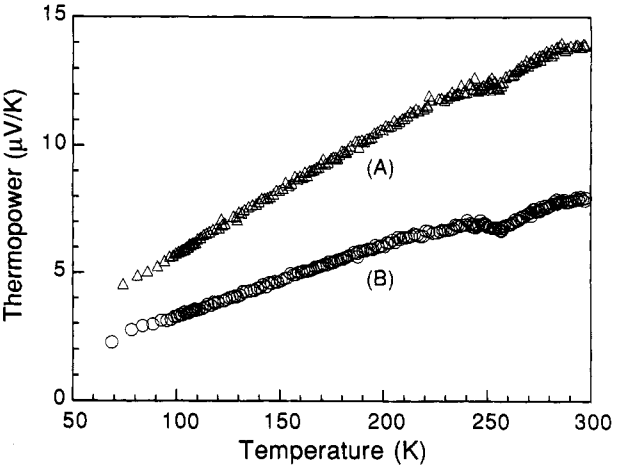

Figure 17. Variable-temperature thermoelectric power data for poly(DBTT) doped with ferric chloride: (A) fraction I; (B) fraction II.

of the electrical conductivity data, with $\alpha = {}^1/_2$, are satisfactory for both fractions. However, for $\alpha = {}^1/_4$, a satisfactory fit is obtained for fraction II but not for fraction I; see Figure 16. In fact, for fraction II, the fit is slightly better when $\alpha = {}^1/_4$. The fact that $\alpha \neq 1$ rules out band conduction and activation type diffusion, in agreement with the behavior of other polythiophenes.[38] It must be noted that several conduction models can be described with $\alpha = {}^1/_2$, such as carrier tunneling between small metallic particles in an insulating matrix,[36,37] one-dimensional variable range hopping (1D-VRH) between localized states[37] and the Coulomb gap model for certain disordered systems.[39] Three-dimensional variable range hopping (3D-VRH) is described by $\alpha = {}^1/_4$. We therefore see that at least fraction I diverges from the 3D-VRH model. However, using conductivity data alone, one cannot distinguish between the various charge-transport models in granular materials. A complementary probe to address this issue

(35) Mott, N. F.; Davies, E. A. In *Electronic Processes in Non-Crystalline Materials*; Clarendon: Oxford, 1979.
(36) (a) Abeles, B.; Sheng, P.; Coutts, M. D.; Arie, Y. *Adv. Phys.* **1975**, *24*, 407–461. (b) Sheng, P. *Phys. Rev. B: Condens. Matter* **1980**, *B21*, 2180–2195. (c) Sheng, P.; Abeles, B.; Arie, Y. *Phys. Rev. Lett.* **1973**, *31*, 44–47.
(37) Isotalo, H.; Stubb, H.; Yli-Lahti, P.; Kuivalainen, P.; Österholm, J.-E.; Laasko, J. *Synth. Met.* **1989**, *28*, C461–C466.
(38) (a) Masubuchi, S.; Kazama, S.; Mizoguchi, K.; Honda, M.; Kume, K.; Matsushita, R.; Matsuyama, T. *Synth. Met.* **1993**, *55–57*, 4962–4967. (b) Barta, P.; Niziol, S.; Zagorska, M.; Pron, A. *Synth. Met.* **1993**, *55–57*, 4968–4972.
(39) Efros, A. L.; Shklovskii, B. I. *J. Phys.* **1975**, *C8*, L49.
(40) The increased scatter in the data for 12% I_3^- doping results from the large resistance of the sample at low temperature.

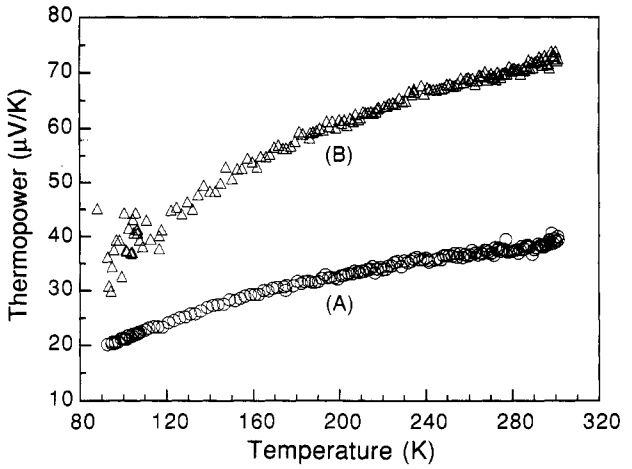

Figure 18. Variable-temperature thermoelectric power data for bulk poly(DBTT) doped with iodine: (A) poly(DBTT)$(I_3^-)_{0.33}$; (B) poly(DBTT)$(I_3^-)_{0.12}$.[40]

is variable temperature thermoelectric power (TP) measurements.

Thermoelectric Power Studies. TP measurements are typically far less susceptible to artifacts arising from the resistive domain boundaries in the material because they are essentially zero-current measurements, and temperature drops across such boundaries are much less significant than voltage drops.

The 1D-VRH hopping model and the Coulomb gap disordered model predict a temperature independent TP, while the carrier tunneling between small metallic particles model predicts a small TP with a linear temperature dependence, where TP approaches zero at 0 K.

Thermoelectric power measurements (Seebeck coefficient) for the two doped (with $FeCl_4^-$) fractions give small positive values in the temperature range 70–300 K, as shown in Figure 17. The thermopower data of the corresponding iodine doped samples are shown in Figure 18. It is clear that both samples exhibit a positive Seebeck coefficient at 300 K which decreases linearly with falling temperature. This is characteristic of a metallike systems in which hole conductivity (p-type) is dominant, as expected from partially oxidized systems. None of the samples show temperature-independent TP, and this excludes the possibility of 1D-VRH and Coulomb gap disordered model. Therefore, it appears that only carrier tunneling between small metallic particles is consistent with the TP data. Similar behavior has been observed in other doped P3AT.[38]

Conclusion

We have demonstrated that a judicious choice of monomer can lead to new highly conductive polythiophene derivatives with long effective conjugation lengths, small number of spin carrying defects, and regular linear backbone. Despite the relatively short chain length, poly(DBTT) is one of the most thermally stable poly(alkylthiophenes). In solution and in the solid state it appears to possess one of the longest chain conjugation lengths among polythiophenes, a result of fewer steric repulsions exerted on its backbone.

Acknowledgment. Financial support from the National Science Foundation (DMR-89-17805) and the Beckman Foundation is gratefully acknowledged. At Northwestern University this work made use of Central Facilities supported by the NSF through the Materials Research Center (DMR-91-20521). The NMR data were obtained on intrumentation that was purchased in part with funds from NIH Grant 1-S10RR04750, NSF Grant CHE-88-00770, and NSF Grant CHE-92-13241. We thank Rabin Bissessur for help with the ESR spin quantitations. We thank Professor G. J. Blanchard for fruitful discussions.